Superconducting-gap symmetry study using a/c boundary Josephson junctions in $YBa_2Cu_3O_{7-\delta}$ films

Yoshihiro Ishimaru, Jianguo Wen, Naoki Koshizuka, and Youichi Enomoto
Superconductivity Research Laboratory, International Superconductivity Technology Center, 1-10-13 Shinonome, Koto-ku, Tokyo 135, Japan
(Received 4 November 1996)

We have investigated gap symmetry of high-T_c superconductors using Josephson junctions formed along a boundary of an a-axis-oriented $YBa_2Cu_3O_{7-\delta}$ (YBCO) grain surrounded by c-axis-oriented YBCO grains (a/c boundary). There are two types of a/c boundary junctions; one is the boundary between (001) of a-axis-oriented grains and (100) of c-axis-oriented grains, and the other is the boundary between (001) of a-axis-oriented grains and (110) of c-axis-oriented grains. TEM observation shows clean, sharp, and nearly single-facet interface along the grain boundaries in both types. In the case of the (100)-(001) type a/c boundary junction, typical resistively shunted junction (RSJ)-type I-V curves, Shapiro steps under microwave irradiation, and Fraunhofer-like diffraction pattern of I_c under magnetic field are observed, indicating that the boundary works as a Josephson junction. In the case of the (110)-(001)-type a/c boundary junction, typical RSJ type I-V curves and Shapiro steps under microwave irradiation are also observed. However, the diffraction pattern of I_c under magnetic field has the minimum value at zero magnetic field. This property is analogous to one observed for a corner junction which is formed between Pb and YBCO. These results show that the (110) of YBCO has a phase difference of π and $d_{x^2-y^2}$ superconducting-gap symmetry is in CuO_2 planes of YBCO. But, the (001) of YBCO has no phase difference of π in spite of the existence of d-wave symmetry in YBCO. [S0163-1829(97)05317-4]

INTRODUCTION

In the high-T_c oxide superconductors, the emerging possibility of d-wave symmetry of the pairing state has attracted wide attention because this seems strongly to imply a mechanism different from the phonon mechanism of the conventional BCS superconductors. Furthermore, this mechanism gives the possibility of new superconductors with higher T_c and brings about some evolution for device application. From this viewpoint, many investigations have been done. To observe the symmetry, Wollman *et al.* used dc-superconducting quantum interference devices (SQUID's) consisting of $YBa_2Cu_3O_{7-\delta}$ (YBCO) and conventional s-wave superconductor Pb.[1] However, it has been pointed out that experiments using the SQUID are susceptible to some fluctuations caused by residual magnetic field, flux trapping, and geometrical symmetry of the SQUID.

To make symmetry of high-T_c superconductors clearly, several researchers used a single Josephson junction consisting of YBCO and Pb.[2–4] If YBCO has an s-wave symmetry, magnetic-field (B) dependence of critical current (I_c) for the Josephson junction shows the conventional Fraunhofer pattern which has a peak at zero field. On the other hand, if it has a d-wave ($d_{x^2-y^2}$) symmetry, B dependence of I_c (I_c-B) for the Josephson junction including a phase difference of π shows the unconventional pattern which has a dip at zero field. Wollman *et al.* observed I_c-B with a dip at zero field for the Josephson junction named a corner junction consisting of (100) and (010) of a YBCO single crystal and Pb.[4] This was considered as evidence for d-wave ($d_{x^2-y^2}$) symmetry. These corner junction properties were also analyzed theoretically as $d_{x^2-y^2}$ symmetry by Tanaka.[5] On the other hand, Sun *et al.* observed a conventional Fraunhofer pattern which has a peak at zero field for a Josephson junction consisting of (001) of YBCO and Pb.[2] This gave evidence for s-wave symmetry. Consequently, we cannot determine the gap symmetry by these experiments.

There is little information about the atomic order roughness or flatness of the interface between YBCO and Pb. This atomic order roughness or flatness is, however, important to determine the superconducting gap symmetry by using Josephson junction because of strong anisotropy of the crystal structure. Furthermore, there are oxidization and deoxidization reactions between the metal Pb and the oxide YBCO, which may cause ambiguity of the gap symmetry. In addition, measurement temperature is limited by the narrow range below T_c of Pb ($=7.2$ K).

In order to study superconducting-gap symmetry of high-T_c superconductors by using Josephson junctions, we should use a junction with an atomic scale flat interface. Many types of Josephson junctions fabricated by various methods have been studied,[6–9] including Josephson junctions using grain boundaries.[10–14] Among them, Josephson junctions using naturally grown grain boundaries between a-axis- and c-axis-oriented grains in YBCO films (we call them a/c boundaries) are interesting, because the atomic scale flat interfaces of the a/c boundaries can be expected by natural formation. Furthermore, two types of a/c boundary junctions are formed; one is the boundary between (001) of a-axis-oriented grains and (100) of c-axis-oriented grains,[15,16] and the other is the boundary between (001) of a-axis-oriented grains and (110) of c-axis-oriented grains.[17]

In this paper, we report microscopic grain-boundary structures and some basic electrical properties for the two types of a/c boundary junctions of YBCO. Especially, the most interesting point in this work is that important information on

superconducting-gap symmetry in YBCO can be obtained by comparing the properties between the two types of a/c boundary junctions.

EXPERIMENT

c-axis-oriented YBCO films including a few a-axis-oriented needlelike grains were fabricated on MgO(001) substrates by pulsed laser deposition. A KrF laser (emission wavelength=248 nm) with power density of about 2 J/cm^2 on stoichiometric high-density targets and the repetition rate of 5 Hz were used as sources. Films of about 200 nm in thickness were grown in oxygen pressure of 200 mTorr at substrate temperature of 780 °C. These conditions are almost the same as those for perfect x-axis-oriented films except for defective substrates. We used the MgO substrate without any annealing treatment to get high-quality films. It is well known that a-axis-oriented grains of YBCO films are fabricated by decreasing the growth temperature, following inferior crystallinity and superconducting properties.[18] In this work, however, we can get the a-axis-oriented needlelike grains in the c-axis-oriented films without decreasing the growth temperature and particular post annealing.

Structures of the films were appraised by x-ray diffraction (XRD) and atomic force microscopy (AFM). Transmission electron microscopy (TEM) samples were prepared for both planar and cross-sectional views to obtain a whole image of a needlelike grain. Electric properties of the grain boundary were observed by a constricted electrode across the boundary. The constricted line with a length of 30 μm and a width of 5 μm were fabricated by photolithography and the Ar-ion-milling technique. In addition, the focused Ga^+ ion-beam (FIB) technique was sometimes used to fabricate the pattern including only one a-axis-oriented grain in the constricted line. I-V characteristics were measured by the usual four-probe method under microwave and magnetic field from 4.2 K to T_c. Magnetic field was applied perpendicular to the film surface by a solenoid coil.

EXPERIMENTAL RESULTS

Microstructure

In our films, grains with a needlelike shape were observed from a topview of thin films. Figure 1(a) shows an optical microscopy surface image of our sample for I-V measurement. The needlelike grains have a length of 5–20 μm and a width of about 200 nm. Most of the direction of the long side is parallel to [100] or [010] of the MgO substrate. There are a few needlelike grains whose direction of the long side is parallel to [110] of the MgO substrate. Figure 1(b) shows an optical microscope surface image of the sample with [110]-type needlelike grains. From the AFM image, the needlelike grains stuck out of the planar parts of the films as pointed protrusion to a height of 100 nm above the surface.

The XRD pattern of the film shown in Fig. 2 consists of only two kinds of diffraction peaks: strong peaks (00i) from the c-axis-oriented grains and weak ones (m00) from the a-axis-oriented grains. No observation of other diffraction peaks except for the MgO substrate means that most of the needlelike grains are of the a-axis orientation in the entire film.

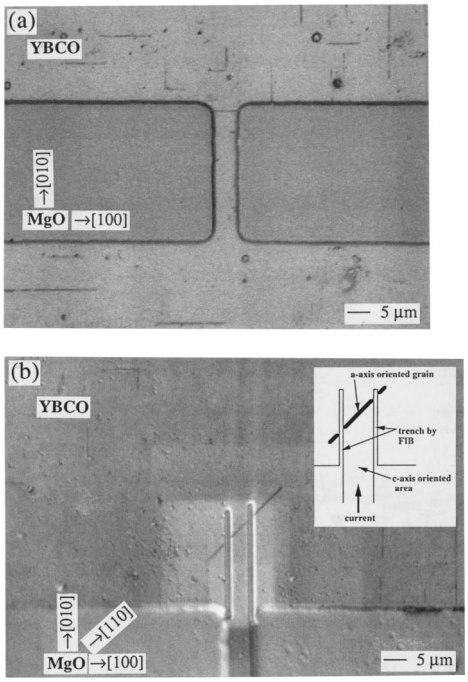

FIG. 1. Micrograph image of the (100)-(001)-type a/c boundary junction (a), and the (110)-(001)-type a/c boundary junction (b). Bridge size with length of 30 μm and width of 5 μm. The inset of (b) is a schematic illustration of the sample which was fabricated by focused-ion-beam (FIB) technique.

Figure 3 shows plane-view and cross-sectional lattice images of a needlelike grain being parallel to [100] or [010] of the MgO substrate by TEM. These images show that the needlelike grain is an a-axis-oriented single crystal and has tabular habit vertical to the substrate. Their dominant epitaxial relationship with respect to the c-axis-oriented regions is [100] a-axis-oriented grain ∥[001] c-axis-oriented grain, and [001] a-axis-oriented grain ∥[100] c-axis-oriented grain. Consequently, the interface structure of the boundaries are formed with (100) and (001) YBCO surfaces. We call this type of grain boundary the (100)-(001)-type a/c boundary. There is a little lattice mismatch between these directions, but TEM revealed well defined, straight grain boundaries without any dislocations and any particulates. This clean in-

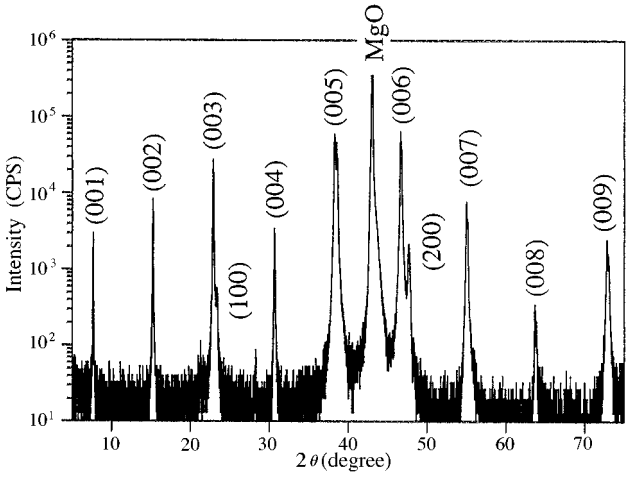

FIG. 2. XRD diffraction pattern of the film.

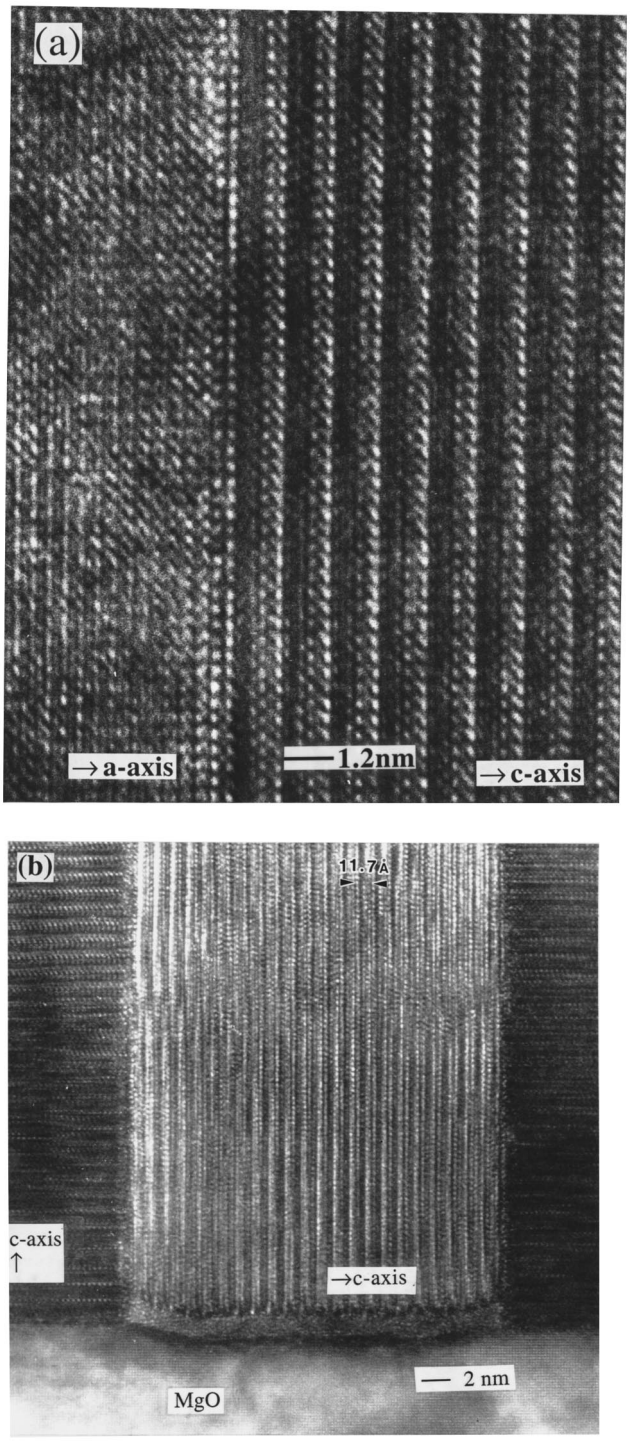

FIG. 3. Plane-view (a) and cross-sectional (b) TEM images of the (100)-(001)-type a/c boundary between a-axis- and c-axis-oriented YBCO grains.

terface is different from the a/c boundary fabricated on an artificially modulated substrate, in which there is some roughness on a microscopic scale.[13] The cross-sectional TEM image of Fig. 3(b) shows that the a-axis-oriented grain grows over the surface of films from about 1 nm thick amorphous layer on the substrates. Consequently, this structure indicates that the superconductive current must flow through this grain because the amorphous layer is not superconducting.

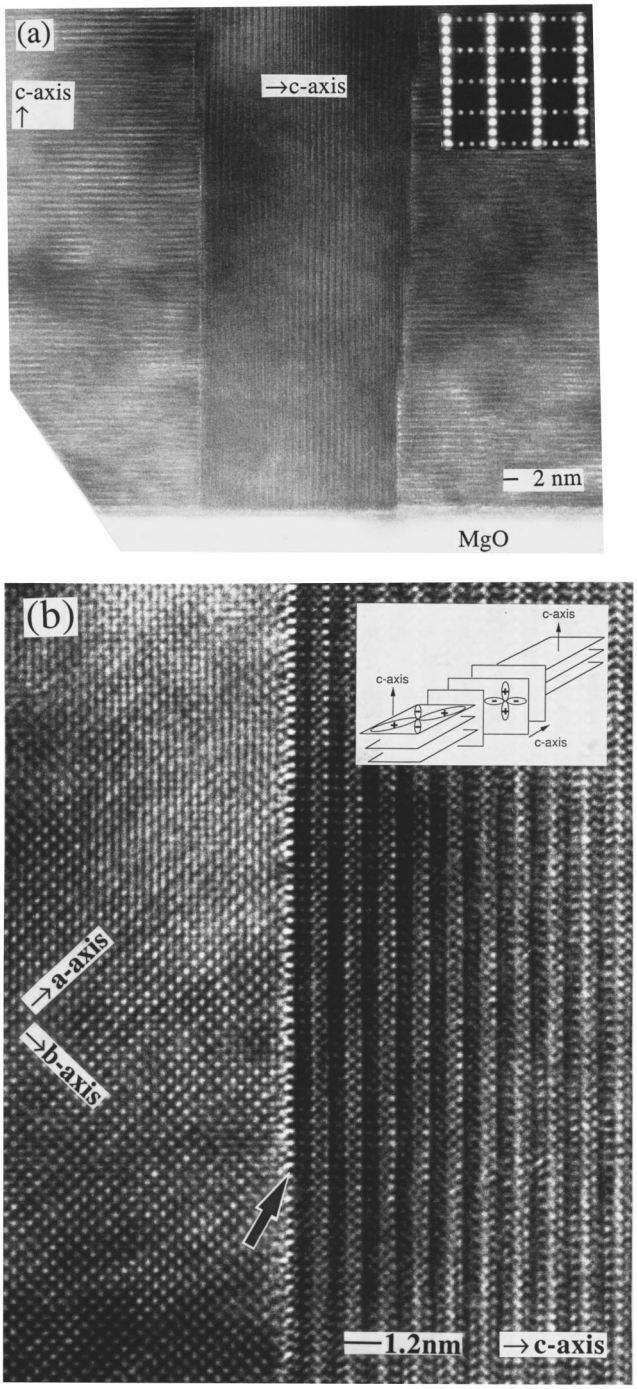

FIG. 4. Cross-sectional (a) and plane-view (b) TEM images of the (110)-(001)-type a/c boundary between a-axis- and c-axis-oriented YBCO grains. The inset in (a) is the electron-diffraction pattern which comes from both grains. The inset (b) is the schematic structure of these grains. The arrow in (b) shows the grain boundary between (001) of the a-axis-oriented grain and (110) of the c-axis-oriented grain.

Figure 4 shows plane-view and cross-sectional lattice images of a needlelike grain being parallel to [110] of the MgO substrate by TEM. The grain is also an a-axis-oriented single crystal. The cross-sectional image shows that the needlelike grains grow right on the substrate. These microstructures are the same as in the [100]-type needlelike grains except for their directions. Their dominant epitaxial relationship with

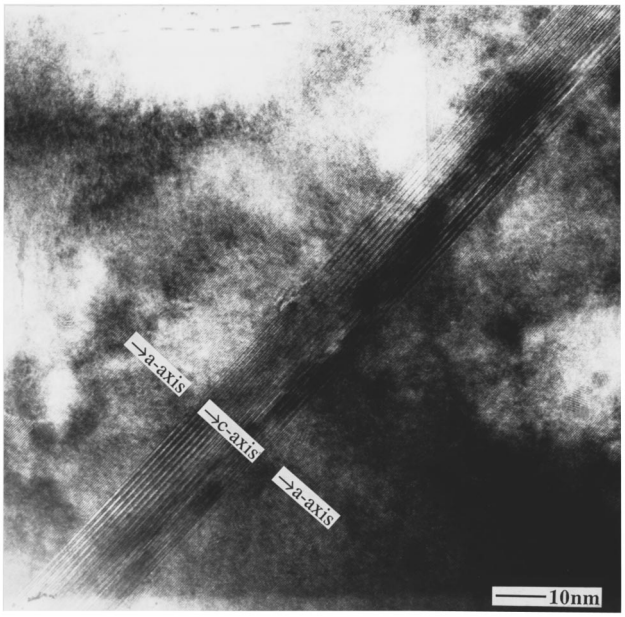

FIG. 5. Wider plane-view TEM image of the (100)-(001)-type a/c boundary between a-axis- and c-axis-oriented YBCO grains.

respect to the c-axis and a-axis-oriented regions is a [100] a-axis-oriented grain $\|$[001] c-axis-oriented grain, and a [001] a-axis-oriented grain $\|$[110] c-axis-oriented grain. This epitaxial relationship is also confirmed from the electron-diffraction pattern in Fig. 4(a) which comes from both of the grains. Consequently, the interface structure of the boundaries formed with (110) and (001) YBCO surfaces. We call this type of grain boundary the (110)-(001)-type a/c boundary. The interface structure of the boundaries is 90° basal-plane-faced tilt boundary in addition to 45° rotation about the [001] in the c-axis-oriented area. The schematic structure of these grains is shown in the inset of Fig. 4(b). In the plane-view image, there is a large lattice mismatch $(1:\sqrt{2})$ between (100) or (010) in the a-axis grain and (110) in the c-axis grain along the boundary. This interface, however, shows a rather clean microstructure without large size dislocation. But the distortion due to the mismatch is only localized in one or two atomic layers at the interface. This type of a-axis-oriented grain growth is supported by a MgO substrate on which 45° tilt grains are observed sometimes.[19]

These two types of a/c boundary junctions are the most suitable for studying superconducting wave-function symmetry by Josephson junction, because they have atomic scale flat interfaces shown by TEM. Figures 3 and 4 only show local area structures, but actually a wider area also shows the same sharp interface shown by a plane-view TEM image in Fig. 5. Even in a wide range image of the (100)-(001)-type a/c boundary, an atomic scale flat interface is realized.

Plane-view TEM observation also shows that there are twin boundaries in c-axis-oriented films for both types. Therefore, on an a/c boundary junction structure, an a-axis-oriented needlelike grain is across these twin boundaries in c-axis-oriented film. However, there are no twin boundaries in a-axis-oriented needlelike grains for both types. This is because, grain boundaries by twins have never been observed in plane-view or cross-sectional TEM images of needlelike grains.

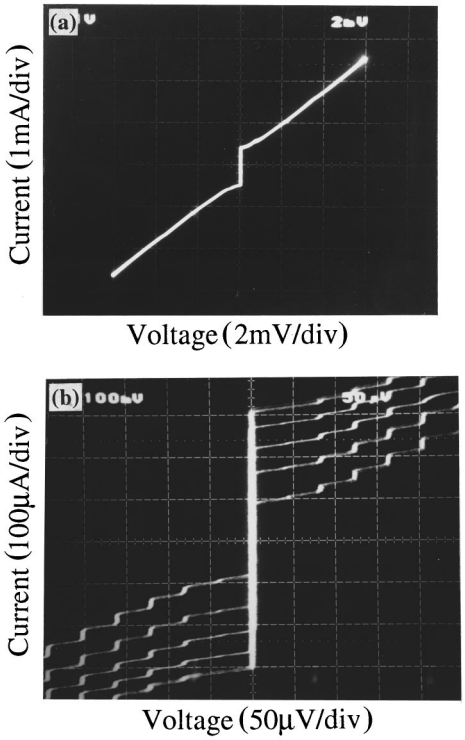

FIG. 6. I-V characteristics of the (100)-(001)-type a/c boundary junction at 28 K (a), and I-V characteristics under 19.49 GHz microwave irradiation of different power at 4.2 K (b).

Finally, we mention why atomic scale flat interfaces are formed along the a/c boundaries. An a-axis-oriented grain grows preferentially along a line-type microstep. Actually, the TEM image in Fig. 3(b) shows existence of a small step of MgO at the bottom edge of the a-axis-oriented grain. After the a-axis-oriented seed layer is formed, the a-axis-oriented grain grows epitaxially on it. In addition, the higher growth rate of the a axis than the c axis makes the a-axis-oriented grains stick out of the c-axis-oriented plain surface. Consequently, the c-axis-oriented films start or stop growing at both walls of the a-axis-oriented grain and surround it. Thus, the atomic scale flat interface perpendicular to the substrate is formed even if mismatch is large. However, we should mention the occurrence of a stacking fault in the a-axis-oriented needlelike grain, although it is not observed in our cross-sectional TEM images. According to this model, a-axis grains start to grow from both sides of line-type microgrooves on the substrates. In this case, the stacking fault is generated at the center of the grain and may work as a Josephson junction. This type of stacking fault was actually observed in a-axis-oriented needlelike grains and reported by other researchers[20] as well as in the plane-view images.[28]

I-V characteristics

The T_c of an electrode including the (100)-(001)-type a/c boundary is about 80 K. This value is not so low for a-axis-oriented films. This rather high T_c is caused by the growth temperature of 780 °C which is higher than conventional growth temperature below 700 °C for a-axis-oriented YBCO films.[21] Figure 6(a) shows an I-V curve at 28 K for

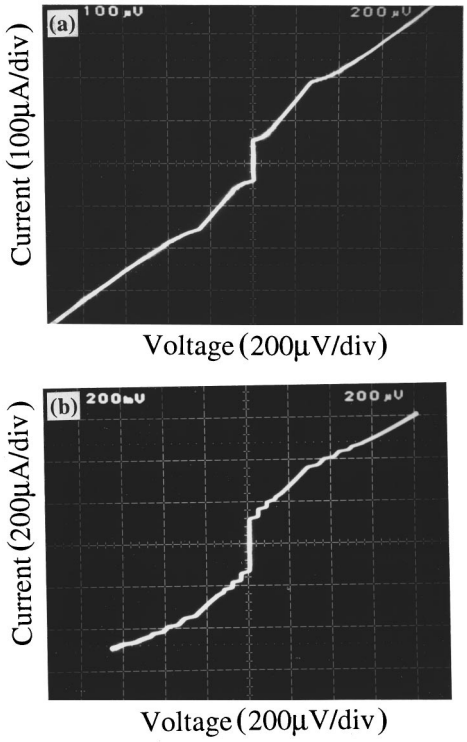

FIG. 7. I-V characteristics of the (110)-(001)-type a/c boundary junction at 4.2 K (a) and I-V characteristics under 19.68 GHz microwave irradiation on the (110)-(001)-type a/c boundary junction at 4.2 K (b).

the (100)-(001)-type a/c boundary formed through only one needlelike grain as shown in Fig. 1(a). Typical resistively shunted-junction (RSJ) characteristics are observed. The value of J_c is 4.4×10^4 A/cm^2 at 4.2 K. Through the current path, two kinds of Josephson junctions can be formed: two Josephson junctions correspond to a/c boundaries, and many Josephson junctions related to intrinsic interlayer between CuO_2 planes in the a-axis-oriented grain. The observed J_c value of 4.4×10^4 A/cm^2 is about two orders smaller than the value 3–5×10^6 A/cm^2 obtained for an a-axis-oriented YBCO film at 4.2 K.[18,21] This result means that the observed weak-link characteristics describe the properties at the interface between a-axis- and c-axis-oriented grains, but not the interplane of the CuO_2 planes. There should be a bend in the I-V curve, if both side junctions of the grain have different critical current. Therefore, no bend in Fig. 6(a) indicates that two a/c boundary Josephson junctions have the same I_c, which is plausible due to the same structure on atomic scale.

Figure 6(b) shows Shapiro steps in I-V curves of the (100)-(001)-type a/c boundary junction under various microwave powers of 19.49 GHz at 4.2 K. These clear Shapiro steps show the (100)-(001)-type a/c boundary works a role of the Josephson junction. I_cR_n product is estimated to be 1.37 mV from the microwave power dependence of Shapiro-step height using the current source model.[22] This value is almost the same as one of the high-quality in-plane rotated grain-boundary junctions reported and satisfies the empirical relation between J_c and I_cR_n.[23] Our junction consists of an a-axis-oriented grain with short coherent length perpendicular to the face of the boundary. Therefore, the rather high I_cR_n value means clear interface along the a/c boundary as well as TEM observation. From this I_cR_n and I_c of 560 μA, R_n is calculated to be 2.44 Ω at 4.2 K. This value agrees with R_n of 2.41 Ω obtained by extrapolation to high bias voltage in the I-V curve.

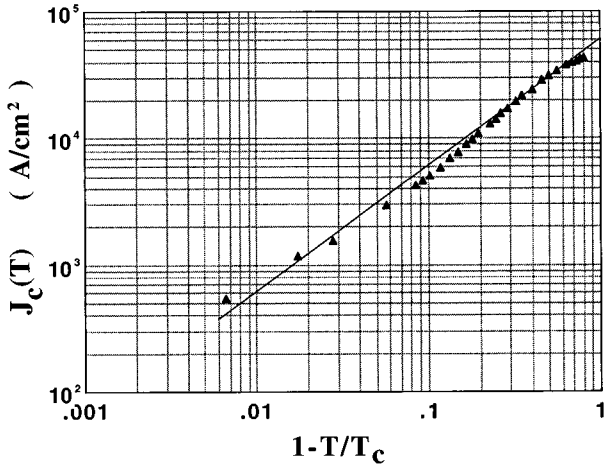

FIG. 8. Temperature dependence of J_c on the (100)-(001)-type a/c boundary junction which is plotted J_c vs $(1-T/T_c)$. The line means that index of the bracket equals 1.

Figure 7(a) shows an I-V curve at 4.2 K for the (100)-(001)-type a/c boundary formed through only one needlelike grain as shown in Fig. 1(b). Current flows through the a-axis grain according to a path limited by two drains which were etched by FIB. There is a bend in the I-V curve, which means that two Josephson junctions with different critical currents, I_c's are formed through the current path. These junctions exist in series and closely to each other in a constricted electrode pattern as shown in Fig. 1(b). Both the junctions exhibit typical RSJ-type characteristics. Figure 7(b) shows Shapiro steps in the I-V curves of the (110)-(001)-type a/c boundary junction under microwave of 19.68 GHz at 4.2 K. Two groups of Shapiro steps are observed corresponding to each junction. This result indicates that both junctions play the role of the Josephson junction. As mentioned already, there are two boundaries along both the sides of the a-axis-oriented grain. Therefore, the two junctions observed in the I-V curve are expected to correspond to these grain boundaries. But its probability is low because of different magnetic-field dependence of I_c described later. From the microwave power dependence of the height of Shapiro steps, normal resistance of the junction, R_n, is estimated to be about 2Ω for the lower I_c junctions. In spite of large lattice mismatch density along the boundary, this value of R_n is as low as one of the (100)-(001)-type a/c boundary junction. This means that resistivity along the boundary is independent of misfit density.

Figure 8 shows a critical current density (J_c) of the (100)-(001)-type a/c boundary junction as a function of temperature. J_c can be observed from 4.2 K to about 80 K which is T_c of the samples. Near T_c, the behavior of J_c can be fit by the functional form $J_c\propto(1-T/T_c)$. Generally, the index of the bracket near 1 means formation of the SIS-type junction, which exhibits hysteresis in an I-V curve.[24] In fact, hysteresis I-V curves were reported for some a/c boundary Josephson junctions.[15] For our sample, no hysteresis structure has been observed yet. A similar inconsistent relation be-

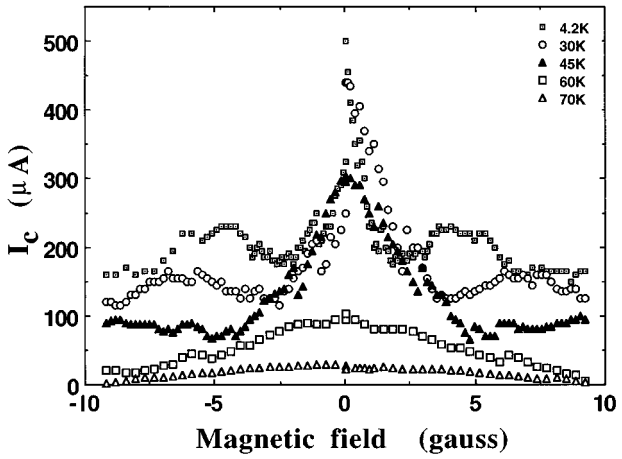

FIG. 9. Magnetic-field dependence of I_c on the (100)-(001)-type a/c boundary junction at various temperatures.

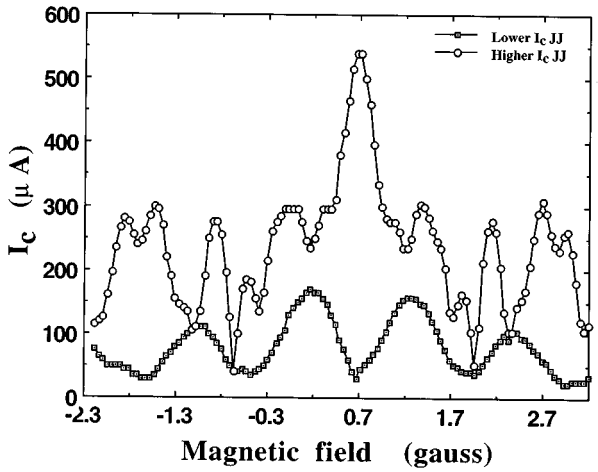

FIG. 10. Magnetic-field dependence of I_c on the (110)-(001)-type a/c boundary junction at 18 K. Minimum I_c value in lower I_c junction occurred at zero magnetic field. This magnetic-field dependence of I_c is analogous to one observed for the s-wave–d-wave corner junction consisted with YBCO and Pb.

tween the index and weak-link properties is observed in other experiments.[25,26] Therefore, the correspondence will have to be clear.

Magnetic-field dependence of I_c

Figure 9 shows the magnetic-field dependence of I_c (I_c-B) for the (100)-(001)-type a/c boundary at various temperatures. In order to obtain information on the lateral uniformity of a junction, the magnetic field was applied normal to a substrate. Magnetic interference patterns are observed below T_c. However, the shapes of the diffraction patterns are quite complicated. At low temperature, the oscillations are nearly triangular which are characteristic of long junction behavior.[27] As the temperature rises, the critical current drops and the oscillations become round and wide. The important point for discussing the symmetry of the superconducting gap is that the I_c-B pattern of the (100)-(001)-type a/c boundary junction has a peak at zero magnetic field.

For the (110)-(001)-type a/c boundary, two junctions with different I_c's are observed in Fig. 7(a) and these I_c's sometimes cross each other during changing magnetic field. Therefore, we carefully obtained I_c's from the entire I-V curves to prevent confusion. Figure 10 shows I_c-B patterns for these two junctions. For the junction with higher I_c, a clear symmetric pattern with a center maximum at about 0.7 G and clear side lobes were observed. This pattern looks like a conventional Josephson junction, for which the I_c peak occurs at real zero magnetic field. Therefore, we think there was a residual magnetic field of -0.7 G at the junction area which comes from terrestrial and external magnetism. The pattern for lower-I_c junction is also symmetric, but it has the minimum value at about 0.7 G magnetic field. Assuming that both the junctions with higher-I_c and lower-I_c are under the same magnetic field due to the close position, minimum I_c value occurs at zero magnetic field. This magnetic-field dependence of I_c is analogous to the one observed for the s-wave–d-wave corner junction reported by Wollman *et al.*[4]

In the case of our sample of the (110)-(001)-type a/c boundary, there are three grain-boundary Josephson junctions through the current path; two junctions are formed along two a/c boundaries and one corresponds to the boundary of the stacking fault as mentioned previously. This situation is shown in Fig. 11. In this situation, two a/c boundary Josephson junctions have the same I-V characteristics because these two boundaries are composed of the same structure in atomic scale, and two a/c boundary Josephson junctions behave like only one Josephson junction in I-V characteristics. Thus, two kinds of I_c-B patterns are observed in I-V characteristics; one corresponds to two a/c boundaries behaving like only one junction and the other corresponds to the stacking fault.

In Fig. 12, one set of the higher and lower I_c patterns is observed at low temperature, and another set of the patterns is observed after heating up to room temperature. This unchanging symmetry of the patterns shows that the diffraction pattern with a dip at zero magnetic field is not caused by the flux trapping generated irregularly.

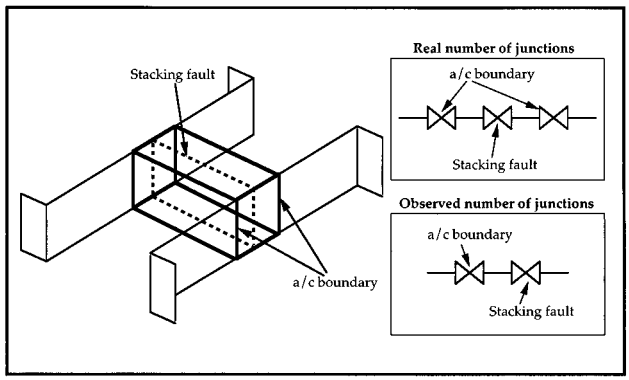

FIG. 11. Schematic structure for our sample of the (110)-(001)-type a/c boundary. There are three grain boundaries through the current path; two junctions are formed along two a/c boundaries and one corresponds to the stacking fault. Two a/c boundary Josephson junctions have the same I-V characteristics because these two boundaries are composed of the same structure in atomic scale, and two a/c boundary Josephson junctions behave like only one Josephson junction in I-V characteristics.

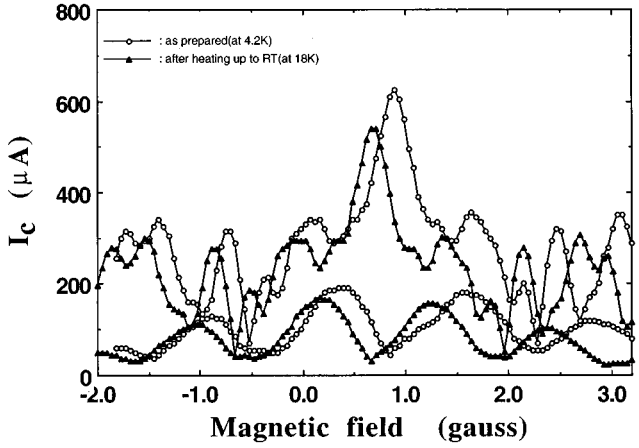

FIG. 12. Temperature dependence of the magnetic-field dependence of I_c patterns with peak and dip at zero magnetic field at different temperature on the (110)-(001)-type a/c boundary junction. As prepared (1), after heating up to room temperature (2).

We have observed I_c-B with the dip at zero magnetic field for another (110)-(001)-type a/c boundary junction. On the other hand, this type of I_c-B pattern has never been observed in the junctions using the (100)-(001)-type a/c boundary. Therefore, we believe this pattern of lower I_c junction is caused along the grain boundary between (110) of the c-axis-oriented grain and (001) of the a-axis-oriented grain. As a result, the higher-I_c junction is formed along a stacking fault in the a-axis-oriented grain.

Figure 13 shows I_c-B patterns for the junction with lower I_c at 4.2, 18, and 36 K. Maximum I_c values decrease with increasing temperature, but symmetry of the patterns is the same. At 36 K, the I_c value at zero magnetic field is suppressed to almost zero.

Figure 14 shows the temperature dependence of I_c for both the (100)-(001) and the (110)-(001) types of a/c boundary Josephson junctions. These two I_c's decrease monotonously with increasing temperature, but they have different temperature dependence. Maximum J_c values at 4.2 K of the (110)-(001)-type a/c boundary junction was 1.4×10^4 A/cm^2. This J_c value is about 1/3 smaller than 4.4×10^4

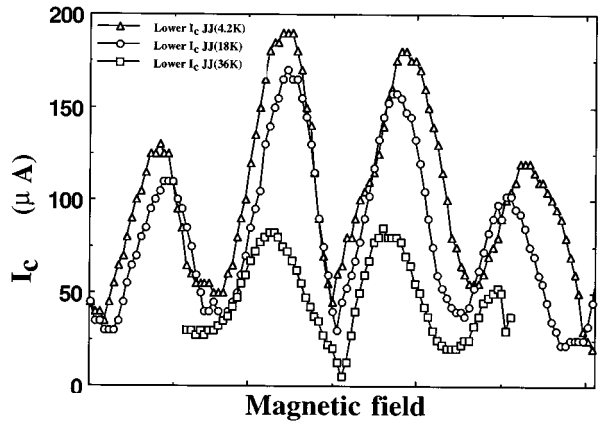

FIG. 13. Temperature dependence of the magnetic-field dependence of I_c patterns at 4.2, 18, and 36 K on the (110)-(001)-type a/c boundary junction with minimum I_c value at zero magnetic field.

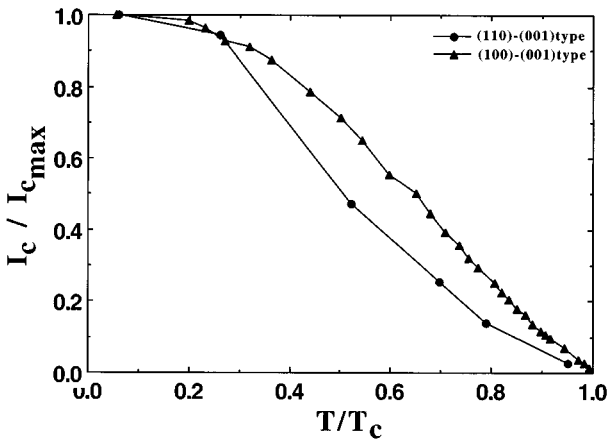

FIG. 14. Temperature dependence of I_c at the (100)-(001)- and the (110)-(001)-type a/c boundary junctions.

A/cm^2 of the (100)-(001)-type a/c boundary junction. This small J_c and different temperature dependence of I_c may be related to the structure difference between the boundaries as well as superconducting-gap symmetry in YBCO.

DISCUSSION

From TEM images, it is clear that the two types of a/c boundary junctions used in this experiment have atomic scale flatness and clear interfaces of the boundaries. In addition, atomic species along both types of the boundaries were determined. BaO layers are terminated at the (001) for both types of a/c boundary.[28] Thus, superconducting-gap symmetry is held at these clear interfaces. We would like to mention again the important role of the flat and clear interface. There are some experiments using grain-boundary Josephson junctions for the superconducting-gap symmetry.[29–31] But, microscale inhomogeneity exists along these grain boundaries fabricated by bicrystal (including tricrystal) and biepitaxial methods,[32,33] and smears I_c-B pattern.

The I_c-B pattern with a dip at zero field has been observed in junctions using the (110)-(001)-type a/c boundary, but never in the (100)-(001)-type a/c boundary. Here, we discuss the size effect on Josephson junctions. A theoretical analysis reports that magnetic-field dependence of I_c should show a peak at zero field for a long Josephson junction even with phase difference of π.[34] Therefore, the I_c-B pattern with a peak at zero field does not mean direct evidence of the s-wave junction. In our experiments, some diffraction patterns were observed with long or small junction behavior for the (100)-(001) a/c boundary junctions by changing temperature and pattern width. But, all of these diffraction patterns show the I_c-B pattern with a peak at zero field. Therefore, we believe that the peak at zero field in the I_c-B pattern is an intrinsic property of the (100)-(001)-type a/c boundary.

In order to discuss superconducting-gap symmetry in YBCO, we summarize our experimental results in Table I, together with the results reported before. The dip at zero field in the I_c-B pattern suggests that the phase difference of π occurs at the boundary of the junction, which is called a π junction. And, if a d-wave symmetry gap is in YBCO, phase difference appears along the points on the face [e.g., (100),

TABLE I. Existence of dip at zero field in I_c-B pattern for various couples of Josephson junctions.

Couple	Existence of dip at zero field in I_c-B pattern
(100)-(001) YBCO	No
(110)-(001) YBCO	Yes
Pb-(001) YBCO	No
Pb-(100) YBCO	No
Pb-corner YBCO	Yes

(110), (001) face]. Junctions consisting of Pb and YBCO edges of the (100) or (010) face have conventional I_c-B patterns.[4,35] This suggests that there is no phase difference of π at the (100) or (010) faces of YBCO, because Pb is an s-wave superconductor. By the way, the (100)-(001)-type a/c boundary junctions have no dip in I_c-B patterns. Therefore, there is also no phase difference of π at (001) of YBCO. This lack of phase difference at (001) is consistent with the experimental results of the Josephson junction consisting of Pb and (001) YBCO which Sun and co-workers reported.[2,36] On the other hand, the I_c-B pattern of the (110)-(001) a/c boundary junction behaves similarly to the π junction which consists of Pb and a corner of the YBCO single crystal.[4,35] This coincidence strongly suggests that there is a phase difference of π at (110),[37] and the $d_{x^2-y^2}$ superconducting-gap symmetry in ab planes of YBCO. Thus, the following two points about the phase for some planes of YBCO are clear.

(1) (001) of YBCO has no phase difference of π.

(2) (110) of YBCO has phase difference of π. This is consistent with the $d_{x^2-y^2}$ superconducting-gap symmetry being in the ab planes of YBCO.

Next, we discuss why the Josephson tunneling along the c direction of YBCO has no phase difference of π under the situation in which the $d_{x^2-y^2}$ superconducting-gap symmetry is in the ab planes of YBCO. It is easier to think that (001) of YBCO is expected to have phase difference of π which occurs by total cancellation of the phase at (001) due to a $d_{x^2-y^2}$ symmetry gap. But actually, our experimental results on the a/c boundary Josephson junctions suggest that the (001) of YBCO has no phase difference of π. This interpretation can explain many experimental results using Josephson junctions with YBCO (edge and corner junctions between YBCO and Pb, junction between Pb and (001) of YBCO, two types of the a/c boundary junctions). Therefore, the mechanism that we need must explain two points about the phase relation mentioned above. In addition, the difference of temperature dependence of I_c between the (100)-(001) and the (110)-(001) a/c boundary must be explained by a theory of the superconducting mechanism. Recently, many researchers have been interested in the Josephson-junction properties along the c direction or gap symmetry of the (001) of YBCO, and some research with theoretical analysis has been reported.[38–41]

CONCLUSION

Two types of a/c Josephson junctions were formed along a boundary of an a-axis-oriented grain surrounded by c-axis-oriented grains of $YBa_2Cu_3O_{7-\delta}$. One has been fabricated along boundaries between (001) of a-axis-oriented YBCO grains and (100) of c-axis-oriented YBCO grains, and the other has been fabricated along boundaries between (001) of a-axis-oriented YBCO grains and (110) of c-axis-oriented YBCO grains. TEM observation shows clear lattice images along the a/c grain boundaries in both types on atomic scale. In I-V characteristics, Shapiro steps under microwave irradiation and the diffraction patterns of I_c under magnetic field were observed in both types, indicating that these boundaries work as Josephson junctions.

In the case of the (100)-(001)-type a/c boundary junction, the conventional magnetic-field dependence of I_c with a peak at zero magnetic field is observed. In the case of the (110)-(001)-type a/c boundary junction, the diffraction pattern of I_c under magnetic field has the minimum value at zero magnetic field. These results show that the (110) of YBCO has a phase difference of π and $d_{x^2-y^2}$ superconducting-gap symmetry is in CuO_2 planes of YBCO. But, the (001) of YBCO has no phase difference of π in spite of the existence of d-wave symmetry in ab planes of YBCO. Our experimental results for these a/c boundary Josephson junctions are expected to be analyzed theoretically.

ACKNOWLEDGMENTS

We wish to thank K. Hayashi for preparation of thin films. We would like to thank S. Tanaka for his encouragement and T. Usagawa, K. Saitoh, and K. Tanabe for helpful discussions. This work was supported by NEDO for the R&D of Industrial Science and Technology Frontier Program.

[1] D. A. Wollman, D. J. Van Harlingen, W. C. Lee, D. M. Ginsberg, and A. J. Leggett, Phys. Rev. Lett. **71**, 2134 (1993).
[2] A. G. Sun, D. A. Gajewski, M. B. Maple, and R. C. Dynes, Phys. Rev. Lett. **72**, 2267 (1994).
[3] I. Iguchi and Z. Wen, Phys. Rev. B **49**, 12 388 (1994).
[4] D. A. Wollman, D. J. Van Harlingen, J. Giapintzakis, and D. M. Ginsberg, Phys. Rev. Lett. **74**, 797 (1995).
[5] Y. Tanaka, Phys. Rev. Lett. **72**, 3871 (1994).
[6] J. Gao, W. A. Aarnink, G. Gerritsma, and H. Rogalla, Physica C **171**, 126 (1991).
[7] C. T. Rogers, A. Inam, M. S. Hegde, B. Dutta, X. D. Wu, and T. Venkatesan, Appl. Phys. Lett. **55**, 2032 (1989).
[8] Ch. Neumann, K. Yamaguchi, K. Hayashi, K. Suzuki, Y. Enomoto, and S. Tanaka, Physica C **210**, 138 (1993).
[9] M. S. Dilorio, S. Yoshizumi, K.-Y. Yang, J. Zhang, and M. Maung, Appl. Phys. Lett. **58**, 2552 (1991).
[10] D. Dimos, P. Chaudhari, J. Mannhart, and F. K. Legoues, Phys. Rev. Lett. **61**, 219 (1988).
[11] K. Char, S. Colclough, S. M. Garrison, N. Newman, and G. Zaharchuk, Appl. Phys. Lett. **59**, 733 (1991).

[12] C. L. Jia, B. Kabius, K. Urban, K. Herrmann, G. J. Cui, J. Schubert, W. Zanden, A. I. Braginski, and C. Heiden, Physica C **175**, 545 (1991).
[13] D. J. Lew, Y. Suzuki, A. F. Marshall, T. H. Geballe, and M. R. Beasley, Appl. Phys. Lett. **65**, 1584 (1994).
[14] M. Konishi and Y. Enomoto, Jpn. J. Appl. Phys. **34**, L1271 (1995).
[15] B. M. Moeckly and R. A. Buhrman, Appl. Phys. Lett. **65**, 3126 (1994).
[16] Y. Ishimaru, K. Hayashi, and Y. Enomoto, Jpn. J. Appl. Phys. **34**, L1123 (1995).
[17] Y. Ishimaru, J. G. Wen, K. Hayashi, Y. Enomoto, and N. Koshizuka, Jpn. J. Appl. Phys. **34**, L1532 (1995).
[18] J. F. Hamet, B. Mercey, M. Hervieu, and B. Raveau, Physica C **193**, 465 (1992).
[19] D. H. Shin, J. Silcox, S. E. Russek, D. K. Lathrop, B. Moeckly, and R. A. Buhrman, Appl. Phys. Lett. **57**, 508 (1990).
[20] C. Traeholt, J. G. Wen, V. Svetchnikov, A. Delsing, and H. W. Zandbergen, Physica C **206**, 318 (1993).
[21] S. Mahajan, W. Ito, Y. Yoshida, and T. Morishita, Physica C **213**, 445 (1993).
[22] K. Yamaguchi, K. Suzuki, S. Tanaka, and A. Kawaji, IEICE Trans. C-II, **J77-C-II**, 399 (1994) (in Japanese).
[23] R. Gross, P. Chaudhari, M. Kawasaki, and A. Gupta, Phys. Rev. B **42**, 10 735 (1990).
[24] P. G. De Gennes, *Superconductivity of Metals and Alloys* (Benjamin, New York, 1966).
[25] Y. Fukumoto, S. Hataski, R. Ogawa, and Y. Kawate, Appl. Phys. Lett. **64**, 782 (1994).
[26] H. Suzuki, Y. Fujiwara, Y. Hirotsu, T. Yamashita, and T. Oikawa, Jpn. J. Appl. Phys. **32**, 1601 (1993).
[27] A. Barone and G. Paterno, *Physics and Applications of the Josephson Effect* (Wiley, New York, 1982), Chap. 5.
[28] J. G. Wen, Y. Ishimaru, K. Hayashi, Y. Enomoto, and N. Koshizuka, Mater. Sci. Eng. B **41**, 82 (1996).
[29] J. H. Miller, Jr., Q. Y. Ying, Z. G. Zou, N. Q. Fan, J. H. Xu, M. F. Davis, and J. C. Wolfe, Phys. Rev. Lett. **74**, 2347 (1995).
[30] P. Chaudhari and Shawn-Yu Lin, Phys. Rev. Lett. **72**, 1084 (1994).
[31] J. Mannhart, B. Mayer, and H. Hilgenkamp, Z. Phys. B **101**, 175 (1996); H. Hilgenkamp, J. Mannhart, and B. Mayer, Phys. Rev. B **53**, 14 586 (1996).
[32] C. Traeholt, J. G. Wen, H. W. Zandbergen, Y. Shen, and J. W. M. Hilgenkamp, Physica C **230**, 425 (1994).
[33] C. A. Copetti, F. Ruders, B. Oelze, Ch. Buckal, B. Kabius, and J. W. Seo, Physica C **253**, 63 (1995).
[34] J. H. Xu, J. H. Miller, Jr., and C. S. Ting, J. Supercond. **8**, 649 (1995).
[35] D. A. Brawner and H. R. Ott, Phys. Rev. B **53**, 8249 (1996).
[36] A. G. Sun, A. Truscott, A. S. Katz, R. C. Dynes, B. W. Veal, and C. Gu, Phys. Rev. B **54**, 6734 (1996).
[37] Y. Ishimaru, T. Utagawa, and Y. Enomoto (unpublished).
[38] M. Sigrist, K. Kuboki, P. A. Lee, A. J. Millis, and T. M. Rice, Phys. Rev. B **53**, 2835 (1996).
[39] M. B. Walker, Phys. Rev. B **53**, 5835 (1996).
[40] M. B. Walker and J. Leuttmer-Strathmann, Phys. Rev. B **54**, 588 (1996).
[41] K. A. Muller, J. Phys. Soc. Jpn. **65**, 3090 (1996).